

Combined microCT-microMR imaging in the tridimensional evaluation of bone regeneration

Allegro Conti¹, Raffaele Sinibaldi¹, Sara Spadone¹, Tonino Traini², Giuliana Tromba³, Silvia Capuani⁴, Gian Luca Romani^{1,5}, and Stefania Della Penna^{1,5}
¹Department of Neuroscience, Imaging and Clinical Sciences, G. D'Annunzio Univ. of Chieti and Pescara, Chieti, CH, Italy, ²Department of Stomatolgy and Biotechnologies, G. D'Annunzio Univ. of Chieti and Pescara, Chieti, CH, Italy, ³Elettra-Sincrotrone Trieste S.C.p.A., Basovizza, TS, Italy, ⁴Physics Department, 'La Sapienza' University of Rome, Roma, RM, Italy, ⁵Institute for Advanced Biomedical Technologies (ITAB), G. D'Annunzio Univ. of Chieti and Pescara, Chieti, CH, Italy

Purpose.

Bone damage due to either pathology or trauma is very common. X-ray computed tomography (CT) and classical histological study are usually combined to obtain parameters describing the mechanical structure of the biomaterial and of the newly formed bone. Despite Magnetic Resonance Imaging (MRI) resolution can be worse than CT scan, MRI contrast could produce images showing a richer bone tissue variability compared to CT. We present here a 3D characterization of extracted human jawbone cores based on the co-registration of X-ray Synchrotron Radiation-microCT (SRμCT) and micro-MRI (μMRI) techniques with a new custom-made software^{1,2} and on a clusterization algorithm³ generating a 3D meta-structure of the regenerated bone.

Methods.

A multimodal imaging approach based on μMRI and SRμCT techniques has been applied to study samples of retrieved human jawbone cores in which several millimeters of bovine biomaterials (Bio-Oss bioceramic) were added to support prosthetic restoration. Samples were analyzed by Synchrotron Radiation Micro CT at the SYRMEP beam line at Elettra⁴ with a monochromatic beam of 23 keV in free propagation phase contrast imaging (FPI) (resulting pixel size = 9 μm). T2-weighted μMR images were carried out on a Bruker 9.4 T Avance spectrometer, by using a Multi Slice Multi Echo (MSME) sequence (repetition time TR = 2500 ms, echo time=4.8 ms, matrix 256x256, voxel dimensions 18X18X200 μm³, number of scan NS = 100). The spin-echo decay as a function of TE is described by $S(TE)=S(0)*\exp(-TE/T2^{APP})$, where S(0) is signal at TE=0 and T2^{APP} is the apparent transverse relaxation time, depending on the spin-spin relaxation time T2 and on the Internal Magnetic Field Gradient (IMFG) experienced by protons of gyromagnetic ratio γ^{5,6}. T2^{APP} is given by $\gamma/T2^{APP}=1/T2+1/12(\gamma\text{IMFG TE})^2\text{ADC}$, where ADC is the Apparent Diffusion Coefficient ADC. To co-register SRμCT and μMRI images, an optimized pipeline, using an algorithms based on Normalized Mutual Information, Adaptive Simulated Annealing and 3D floating window approach has been adopted, with a specific attention to manage fit the SRμCT resolution into the worse resolution of the MR images. Transversal sections for histological examination were obtained by cutting the jawbone core after SRμCT and μMRI were recorded. Slice thickness is in the range of 50-90 μm and optical microscopy images have in plane resolution of 1.6 μm. Histological images were obtained after staining the sample with fuchsin dye. Cluster recognition have been obtained through an automated adaptive algorithm on the signals of the Phase Retrieval SRμCT and the T2-weighted signals from the μMRI stacks. A matrix with these measures for all voxels was created and data were clustered through a modified version of the standard K-means procedure³.

Results and discussion.

Figure 1 shows an exemplar slice of a jawbone core acquired with both μMRI (a) and SRμCT (b). SRμCT stack was resampled and registered to match the μMRI one. The gray scale histograms in Figure 1 were calculated over the whole 3D sample volume. Notably, the images and the histograms highlight how the two techniques reveal different phases. In particular, μMRI is able to distinguish the more calcified bone (dark) from the less calcified one (lighter). These phases are characterized by different T2^{APP} relaxation times: with the increasing of the degree of calcification (and so of the density of the matrix), the effects of IMFG on the dephasing of the transverse magnetization and also the effect of the restricted dynamic of water molecules in bone pores increase⁷⁻⁹. μMRI is also able to detect clusters of multinucleate cells while it cannot discriminate between background and the bone marrow. Conversely, SRμCT can detect only one phase of bone (pictured in white), but discriminates void (dark) from marrow (the third peak between background and mature bone distributions). The image in Figure 2 is one of the histological references of our study. This slice, like the others, was taken from the jawbone core by cutting it at a position as close as possible to the corresponding slice imaged by μMRI: this choice was driven by the need to compare the outcome of histology with 3D imaging. Figure 3 shows the 3D meta-structure obtained with the cluster analysis. This method found six different phases, which were labelled according to the histological image: mature bone, newly formed bone and soft newly formed bone (1 and 2, in the figure), soft tissue, multinucleate cells and empty spaces.

Conclusions.

In this paper the 3D morphology and composition of a human jawbone core have been assessed by means of SRμCT and μMRI. These techniques detect complementary features of biological tissues: SRμCT imaging visualizes mineralized tissues with high spatial resolution, while μMRI is sensitive to the presence of mobile hydrogen atoms, which are abundant in water and in the biological macromolecules. Both techniques are well suited to characterize porous-like material and hence the complex bone trabecular structure and in particular calcified tissues by SRμCT, soft or more porous materials from μMRI. We obtained with a data-driven and non-invasive method a cluster pattern very similar to the histological images. Histology confirmed the obtained groups and, in particular, the presence of two different phases of newly formed bone, which were not revealed by μMRI and SRμCT when used as separate imaging tool.

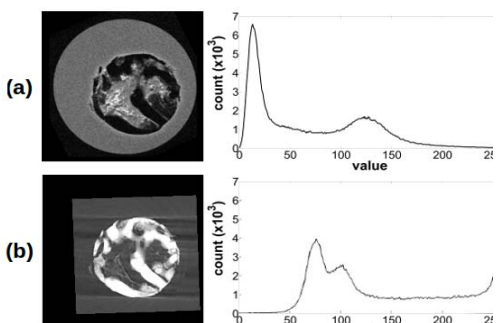


Figure 1: μMRI (a) and SRμCT (b) sample slice of the jawbone. Histograms on the right side were calculated on the entire volume and help to discriminate the different phases detected with both the techniques.

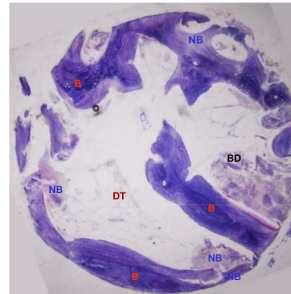


Figure 2: An exemplar image obtained with optical microscopy (resolution 1.6 μm). The picture shows mature trabecular bone (B), newly formed bone (NB), bone debris (BD) and dehydrated soft tissues (DT).

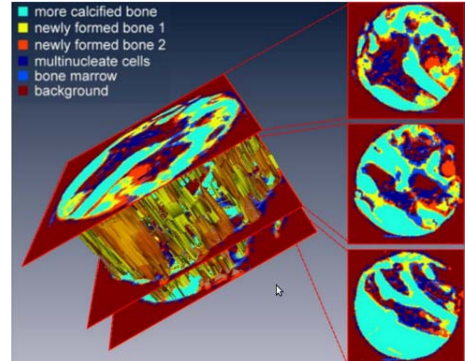


Figure 3: 3D fusion of μMRI and FPI-SRμCT stacks. On the right three slices are pictured and the first corresponds to the histology section shown in Fig.2. On the left, the 3D structure shows the contribution only of the two phases constituting the newly formed bone.

Bibliography: [1] R. Sinibaldi et al. Ann Ist Super Sanita 48, 2012. [2] R. Sinibaldi et al. JBG 2013, Vol. 3, No. 4. [3] S. Spadone et al. Neuroimage 2012;62(3):1912-1923. [4] G. Tromba et al. AIP Conference Proceedings, 1266, 18-23, 2010. [5] S. Majumdar et al. J Magn Reson 1988;78:41-55. [6] H. Y. Carr and E. M. Purcell. Phys Rev 1954; 94:630-8. [7] M. S. Tenner, et al. Invest. Radiol. 1995; 30 (6): 345-353. [8] S. De Santis et al. Phys. Med. Biol. 2010; 55: 5767-5785. [9] F. W. Wehrli. J. Magn. Reson. 2013;229:35-48.